Switchable Total Internal Reflection Light Deflector

Abstract: A new digital light deflector, capable of being switched in less than 35 μ sec with less than 300 V, uses the principle of switchable total internal reflection. The deflector produces high-quality, high-contrast images and its low cost and high light transmittance make it potentially well suited for use in optical-beam-addressable memory systems as well as for other applications in which random deflection is desirable.

Introduction

Current development activity in light-beam-addressable memories has created a demand for high-speed, low-cost digital light deflectors. Deflectors using electro-optic switches, which act as half-wave plates, and polarization-dependent deflecting elements have been described previously. They are, however, quite expensive and, because of the transparent electrodes on the faces of the KDP electro-optic switches, the light transmittance of multistage deflectors of this type is poor.

Asynchronous analog light deflectors employing refraction by prisms made of electro-optic materials, 7-11 diffraction by acoustically generated refractive index variations, 12-15 and reflection by piezoelectrically driven mirrors have also been described. These deflectors are either not capable of producing a sufficient number of resolvable output positions or, when the resolution potential is high, they are too inefficient for many applications.

Scanlasers, which use internal means to control the direction or position of the light emitted by a laser, have been made.^{17,18} However, because a high-gain and high-numerical-aperture laser is required, these techniques can be applied, in a practical way, to only a few lasers at the present time.

For many applications the high-speed capability (about 1 μ sec deflection time) of the electro-optic-switch digital deflector is unnecessary and lower cost and greater light transmittance are required. Additionally, the accuracy and stability afforded by digital deflectors are desirable in systems that require random deflection of the light beam. The light deflector described here is intended to meet these requirements.

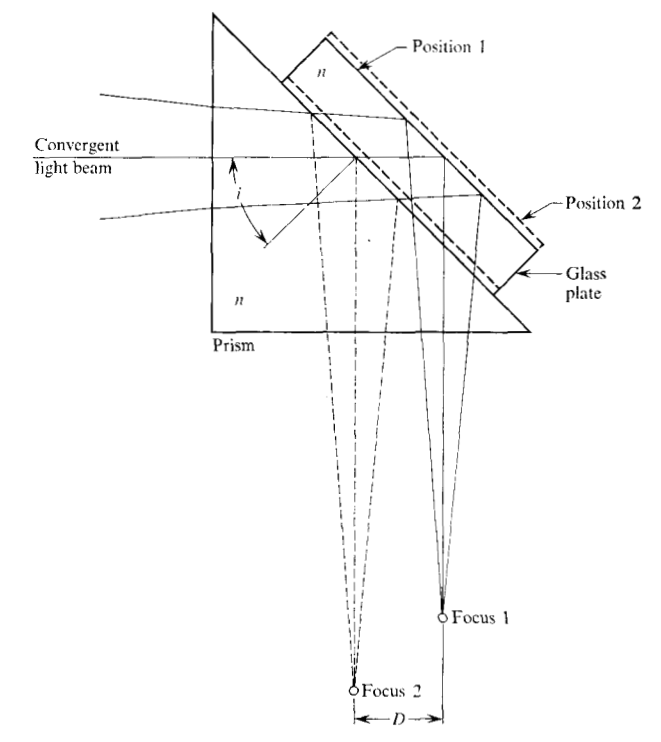


Figure 1 Principle of operation of the light deflector.

Principle of operation

The principle of operation of the light deflector is shown in Fig. 1. When the glass plate is in Position 1, i.e., in optical contact with the prism, the light enters the glass plate and is totally reflected at the back surface. When the glass plate is out of optical contact, as in Position 2 in

179

The author is located at the IBM Systems Development Division Advanced Technology Laboratory, San Jose, California 95114.

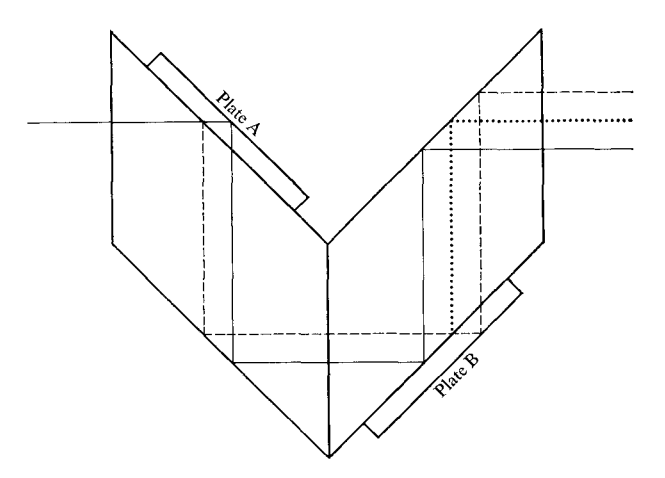


Figure 2 Means for eliminating the longitudinal focus shift. Plates A and B of equal thickness constitute one stage of the deflector. When Plate A is in contact with its prism, Plate B will be out of contact with its prism and vice versa; hence the path length through the prisms is the same for both beams. When used as a focus shifter, both plates are either in, or out of, contact with the prisms; in this case the emerging beam principal ray follows the dotted line.

Table 1 Values of transmittance and reflectance for frustrated total reflection.*

n	i	d/λ	T_{σ}	R_{σ}	T_{π}	R_{π}
1 517	450	0.005	0.0000	0.0002	0.0000	0.0001
1.517	45° 45°	0.005 0.010	0.9998	0.0002 0.0015	0.9999	0.0001
1.517 1.517	45°	0.010	0.9985 0.9941	0.0013	0.9994 0.9975	0.0025
1.517	45°	0.020	0.9869	0.0039	0.9944	0.0023
1.517	45°	0.030	0.9809	0.0131	0.9944	0.0030
1.517	45°	0.040	0.9771	0.0229	0.9847	0.0099
1.517	45°	0.050	0.9499	0.0501	0.9847	0.0133
1.317	43	0.000	0.9499	0.0301	0.9761	0.0219
1.517	45°	1.000	0.0125	0.9875	0.0290	0.9710
1.517	45°	1,200	0,0047	0.9953	0.0110	0.9890
1.517	45°	1.400	0.0017	0.9983	0.0041	0.9959
1.517	45°	1.600	0.0006	0.9994	0.0015	0.9985
1.517	45°	1.800	0.0002	0.9998	0.0006	0.9994
1.517	45°	2.000	0.0001	0.9999	0.0002	0.9998
1.650	45°	0.005	0.9994	0.0006	0.9996	0.0004
1.650	45°	0.010	0.9979	0.0021	0.9984	0.0016
1.650	45°	0.020	0.9914	0.0086	0.9936	0.0064
1.650	45°	0.030	0.9809	0.0191	0.9858	0.0142
1.650	45°	1.000	0.0013	0.9987	0.0018	0.9982
1.650	45°	1.200	0.0003	0.9997	0.0004	0.9996
1.650	45°	1.400	0.0001	0.9999	0.0001	0.9999
1.517	48°	0.005	0.9995	0.0005	0.9997	0.0003
1.517	48°	0.010	0.9983	0.0017	0.9989	0.0011
1.517	48°	0.020	0.9935	0.0065	0.9956	0.0044
1.517	48°	0.030	0.9855	0.0145	0.9900	0.0100
1.517	48°	1.000	0.0038	0.9962	0.0056	0.9944
1.517	48°	1.200	0.0010	0.9990	0.0015	0.9985
1.517	48°	1.400	0.0002	0.9998	0.0004	0.9996

^{*} Two values of index of refraction and two angles of incidence are included to provide a quantitative indication of the dependence of transmittance and reflectance on these quantities. The smaller index n is that of borosilicate crown glass and the larger value represents an extra-dense crown glass.

Fig. 1, the beam is totally reflected at the surface of the prism. Thus a lateral beam displacement D is achieved by switching the position of the glass plate.

In addition to the lateral displacement an unwanted longitudinal focus shift is produced. This shift can be eliminated by using two deflector plates of equal thickness as shown in Fig. 2. When Plate A is in optical contact with its prism, Plate B will be out of contact with its prism and vice versa; hence the total optical path length is invariant with the beam output position. Because of the geometrical arrangement of the plates and prisms, the lateral displacement of the beam produced by Plate B will be added to that produced by Plate A of the same stage.

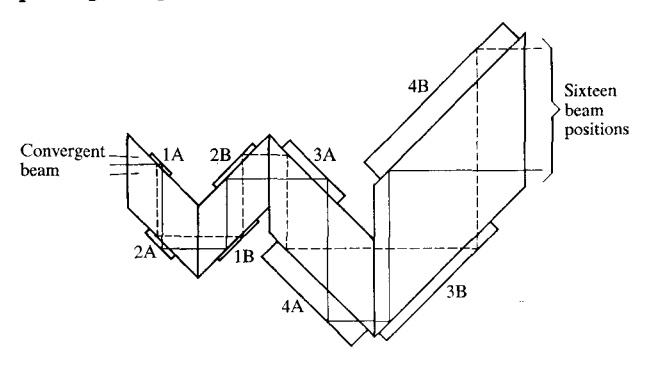
A multistage deflector is composed of a series of parallelogram prisms, each of which is fitted with one or more glass plates. One configuration for a four-stage deflector is shown in Fig. 3. The thickness t_k of the glass plate of the kth stage is given by

$$t_k = 2^{k-1}t_1, (1)$$

where t_1 is the thickness of the glass plate of the first stage of the deflector.

Two-dimensional deflection is possible by using two sets of deflectors oriented to produce deflections at right angles. Deflection in the third dimension (focus shift) can be achieved by operating the A and B plates of one stage so that they are both in, or both out of, optical contact with the prisms. As can be seen in Fig. 2, no lateral deflection is produced when both plates are moved out of contact with their prisms. The decrease in physical path length within the glass is $2t/\cos i$; hence the paraxial focus in air will be shifted by an amount equal to $2t(n-1)/(n\cos i)$. The decrease in path length in glass will result in a decrease in the correction of the longitudinal aberrations and, when the principal ray is not normally incident on the entrance and exit faces of the prisms, an increase in the correction of the lateral aberrations of the system.

Figure 3 Four-stage deflector employing double deflectors per stage for path-length equalization.



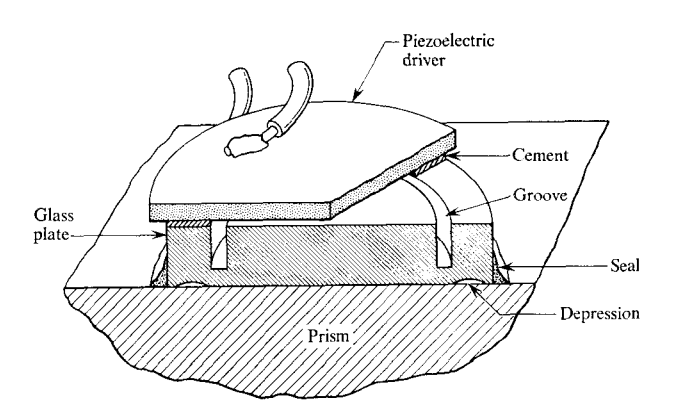


Figure 4 Circular-type deflector showing the glass plate in contact with the prism.



The distance that the glass plates must be driven can be determined from Eqs. (2) and (3), which give the transmittance for frustrated total reflection¹⁹ as illustrated in Fig. 1:

$$T_{\sigma} = \left\{ \frac{(n^{2} - 1)^{2}}{4n^{2}(n^{2} \sin^{2} i - 1) \cos^{2} i} \right.$$

$$\times \sinh^{2} \left[\frac{2\pi d}{\lambda} (n^{2} \sin^{2} i - 1)^{\frac{1}{2}} \right] + 1 \right\}^{-1}; \qquad (2)$$

$$T_{\tau} = \left\{ \frac{(n^{2} - 1)^{2}(n^{2} \sin^{2} i - \cos^{2} i)^{2}}{4n^{2}(n^{2} \sin^{2} i - 1) \cos^{2} i} \right.$$

$$\times \sinh^{2} \left[\frac{2\pi d}{\lambda} (n^{2} \sin^{2} i - 1)^{\frac{1}{2}} \right] + 1 \right\}^{-1}. \qquad (3)$$

Here T_{σ} is the transmittance of the component of plane polarized light with electric vector perpendicular to the plane of incidence, T_{π} is the transmittance of the component with electric vector parallel to the plane of incidence, n is the index of refraction of the plate and prism, d is the separation of the plate and prism, and i is the angle of incidence. Table 1 contains a few values of T_{σ} and T_{π} as well as values of the reflectances R_{σ} and R_{π} , which are calculated from Eqs. (4) and (5):

$$R_{\sigma} = 1 - T_{\sigma}; \tag{4}$$

$$R_{\pi} = 1 - T_{\pi}. \tag{5}$$

From Table 1 it is apparent that the plate-to-prism spacing must be roughly $\lambda/50$ or less when in optical contact and 1.6 λ or greater when out of contact to avoid unwanted secondary output.

It would appear from these data that the interface surfaces of the glass plate and prism must be flat within about $\lambda/50$. However, since rather large forces exist between two glass plates that are in optical contact, by using thin and

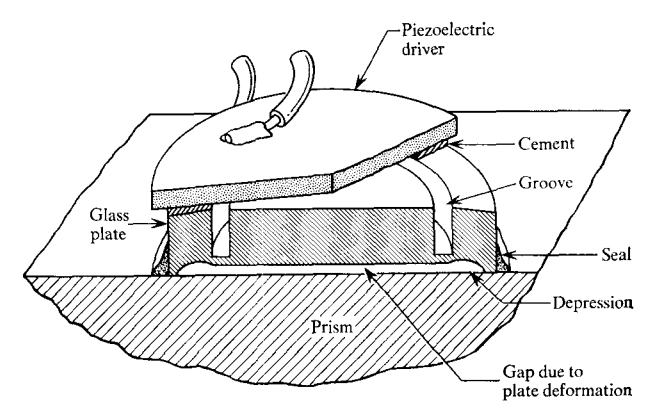
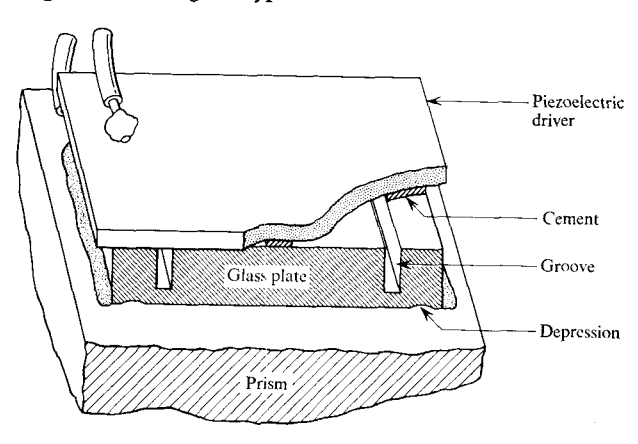


Figure 5 Circular-type deflector showing the glass plate out of contact with the prism. The separation of the plate and prism and the bending of the plate and driver are greatly exaggerated.

Figure 6 Rectangular-type deflector.



therefore deformable plates the interface surfaces of the glass plates and prisms need not be exceptionally flat. Once optical contact is established at some position on the plate, the attractive force pulls the remainder of the plate into contact with the prism. With plates of 3-mm thickness, at least one-half fringe per cm of aperture can be tolerated. Because air must be excluded from the space between the interface surfaces to permit the plate to be moved rapidly into optical contact with the prism, the entire system is either operated in a vacuum or the plate and prism are sealed around the edge while the system is temporarily in a vacuum. Pressures as high as a few cm of mercury can be tolerated.

The method by which the plates are driven in and out of contact with the prisms is illustrated in Figs. 4, 5, and 6. A piezoelectric driver is cemented to the glass plate in the region shown. When a depoling field (polarity opposite that of the initial poling field) is applied, the driver expands radially and causes the glass plate to be

deformed, the central portion of the plate being forced out of contact with the prism. Grooves ground in the surface of the plate that makes contact with the piezoelectric driver weaken the structure so that it can be deformed more easily with a low drive-voltage. Circular plates (Fig. 4) have a continuous groove near the edge and rectangular plates (Fig. 6) have parallel grooves. Depressions are polished in the surface that makes contact with the prism (Figs. 4 and 6) to reduce the area of contact that must be separated. These depressions also form nucleation sites from which the separation of the two surfaces is initiated. Thus the glass plate is peeled off the prism with the separation proceeding inward from the region of the depression. Since the area over which the plate and prism are being separated at any instant of time is greatly reduced by the peeling action, the total force required to separate the plate and prism is also greatly reduced.

The piezoelectric drivers which have been used are lead titanate-lead zirconate ceramics and are available commercially from a number of manufacturers. Piezoelectric deformation normal to the direction of poling of the material is employed; hence the d_{31} constant must be used in calculating the magnitude of the deformation. Different formulations of lead titanate-lead zirconate piezoceramics have different properties; materials with d_{31} constants ranging from about -90 to -270 pm/V have been used. The calculated change in diameter of an unclamped 2-cm diameter disk ranges from 1.35 to 4.05 µm when a potential difference of 300 V is applied across the 0.04-cm thickness. In the configurations used this change in size of the piezoelectric driver is sufficient to produce a separation of the plate and prism in excess of the required 1.6 λ .

The deflectors operate over a range of voltage; therefore well-regulated power supplies are not required. Transistor-or silicon-controlled rectifier circuits with time constants between 1 and 4 μ sec are used to switch the voltage on the drivers. With piezoelectric drivers that have a capacitance of 0.005 μ F (per cm² driver area) the circuits must be capable of delivering peak currents of 1.5 to 0.375 A (per cm² driver area) when a potential difference of 300 V is applied to the driver.

The piezoelectric material, when subjected to an electric field for a period of time, suffers a semipermanent creep. Application of a depoling field (which causes a radial expansion of the disk) results in a semipermanent increase in the diameter of the disk while a poling polarity field produces a semipermanent decrease in diameter. Experiments show that the amount of creep is a nonlinear function of both the duration and the magnitude of the applied field and that the creep is greater for a depoling polarity field than for a poling field of the same magnitude and duration. By operating the driver at field strengths

of not more than 400 V/mm, the magnitude of the creep can be minimized. By biasing the deflector so that the required value of the operating depoling voltage is decreased while the minimum poling voltage is increased, the net creep can be reduced to a negligible amount. The deflector is biased by maintaining a poling polarity field on the piezoelectric driver during the period in which the cement that bonds the driver to the glass plate is curing. Therefore when the voltage is removed the piezoelectric driver expands, tending to lift the center of the glass plate from the prism.

Experimental results

Individual deflector stages have been made with plate diameters ranging from 1 to 5 cm and with plate thicknesses ranging from 0.06 to 0.51 cm. The smallest deflectors switch in about 7 usec while the largest require about 35 μ sec. (Switching time is defined as the interval between the time the voltage across the driver begins to change and the time the deflector is optically in the switched condition.) To achieve these switching times, potential differences of 200 to 300 V are required. Optical transition times range from about 2 to 10 µsec; the remainder of the switching time is required for charging the piezoelectric capacitor and for deforming the driver. To limit the temperature rise in the driver to a few degrees centigrade, experiments have shown that the deflection rate must be limited to about 2000/sec unless special means are provided to cool the piezoelectric driver. With circulating water in contact with the external surface of the driver, 48,000 deflections per second have been achieved.

The ratio of the intensity of light in the useful output to that of the undesired output of a single stage, i.e., the contrast, is dependent on the plate-prism separation as shown in Table 1. When the glass plate is in optical contact with the prism, the separation in most areas of the plate is extremely small and very little light is reflected at the interface between the plate and the prism. However, a few relatively deep pits in the surfaces and small dirt specks can cause local plate-prism separations that limit the contrast. With plates which have a surface polish equivalent to that of quality reticles, contrast of 2000 to 1 or higher is achieved. (When the glass plate is out of contact with the prism, the contrast is usually greater than 5000 to 1.)

Because the glass plate is forced into and out of optical contact with the prism, the life of the deflector is limited by the abrasion of the interface surfaces. To date deflectors have been tested to 2×10^8 deflections. Several ways by which the life of the deflectors can be extended are currently under investigation. These include lubrication of the interface surfaces by thin layers of lubricants, reduction of adhesive forces between plate and prism by means of surface contaminants, reduction of the force with which

the plate strikes the prism by increased gas pressure in the interface region, and the use of flatter and smoother surfaces.

Acknowledgments

The author thanks W. K. Banks, P. Thomas, J. Groot, J. M. Fleischer III, and H. F. Girrbach for valuable contributions in developing this light deflector.

References

- W. Kulcke, T. J. Harris, K. Kosanke, and E. Max, *IBM J. Res. Develop.* 8, 64 (1964).
- 2. T. J. Nelson, Bell System Tech. J. 43, 821 (1964).
- 3. W. J. Tabor, Bell System Tech. J. 43, 1153 (1964).
- W. Kulcke, K. Kosanke, E. Max, H. Fleischer, and T. J. Harris, Optical and Electro-Optical Information Processing, MIT Press, Cambridge, p. 371 (1965).
- R. A. Soref and D. H. McMahon, Appl. Opt. 5, 425 (1966).
- M. A. Habegger, T. J. Harris, and J. Lipp, Appl. Opt. 5, 1403 (1966.)
- V. J. Fowler, C. F. Buhrer, and L. R. Bloom, Proc. IEEE 52, 193 (1964).

- 8. W. Haas, R. Johannes, and P. Cholet, Appl. Opt. 3, 988 (1964).
- F. S. Chen, J. E. Geusic, S. K. Kurtz, J. G. Skinner, and S. H. Wemple, *Proc. IEEE* 52, 1258 (1964).
- R. Kalibjian, T. Kuen, C. Maninger, and J. Yee, Proc. IEEE 53, 539 (1965).
- F. S. Chen, J. E. Geusic, S. K. Kurtz, J. G. Skinner, and S. H. Wemple, J. Appl. Phys. 37, 388 (1966).
- M. G. Cohen and E. I. Gordon, Bell System Tech. J. 44, 693 (1965).
- 13. A. Korpel, R. Adler, P. Desmares, and T. M Smith, IEEE J. Quant. Elec. QE-1, 60 (1965).
- C. F. Quate, C. D. W. Wilkinson, and D. K. Winslow, Proc. IEEE 53, 1604 (1965).
- E. G. H. Lean, C. F. Quate, and H. J. Shaw, Appl. Phys. Letters 10, 48 (1967).
- 16. V. J. Fowler and J. Schlafer, Appl. Opt. 5, 1675 (1966).
- R. V. Pole and R. A. Myers, IEEE J. Quant. Elec. QE-2, 182 (1966).
- R. A. Myers and R. V. Pole, IBM J. Res. Develop. 11, 502 (1967).
- 19. E. E. Hall, Phys. Rev. 15, 73 (1902).

Received July 24, 1968